

Geometry and electronic properties of single vacancies in achiral carbon nanotubes

C. Wang^a and C.Y. Wang

Department of Physics, Tsinghua University, Beijing 100084, P.R. China

Received 21 August 2006 / Received in final form 29 September 2006

Published online 22 December 2006 – © EDP Sciences, Società Italiana di Fisica, Springer-Verlag 2006

Abstract. An ideal single vacancy can be formed by removing one carbon atom from a hexagonal network. The vacancy is one of the most important defect structures in carbon nanotubes (CNTs). Vacancies can affect the mechanical, chemical, and electronic properties of CNTs. We have systematically investigated single vacancies and their related point defects for achiral, single-walled carbon nanotubes (SWNTs) using first-principles calculations. The structures around single vacancies undergo reconstruction without constraint, forming ground-state or metastable-state structures. The 5-1DB and 3DB point defects can be formed in armchair CNTs, while the 5-1DB-P and 5-1DB-T point defects can be formed in zigzag CNTs. The related point defects can transform into each other under certain conditions. The formation energies of armchair CNTs change smoothly with the tube radius, while in the case of the 3DB defect, as the radius get larger, the formation energies tend towards a constant value.

PACS. 61.46.+w – 61.72.Ji Point defects (vacancies, interstitials, color centers, etc.) – 71.15.Mb Density functional theory, local density approximation, gradient and other corrections

1 Introduction

Since their discovery [1], carbon nanotubes have attracted much attention due to their fascinating properties. One of their most attractive aspects is that the CNTs can be either metallic or semiconducting, depending on their intrinsic geometries [2]. Many previous results obtained from both experimental and theoretical research have revealed the novel properties of carbon nanotubes [3–6]. A carbon nanotube was first considered as perfect graphene sheet wrapped up into a cylinder; however, as more experimental results become available and theoretical investigations get deeper, it appears that CNTs are not as perfect as they were once believed to be. Defects such as 5–7 rings, kinks, junctions, vacancies, and impurities [7–11] may be present in CNTs. These defects can significantly change the electronic, chemical, and mechanical properties of the CNTs.

The single vacancy is one of the most important defect structures in CNTs. Amongst various kinds of topological defects in CNTs, it has been studied particularly intensively [8, 19–22]. An ideal single vacancy can be formed by removing one carbon atom from the perfect tube, which could be achieved by electron or ion irradiation [8, 19], leaving three dangling bonds around the vacancy. Vacancies can govern both the electronic [12] and mechanical [13, 14] properties of nanotubes. The work of Robinson et al. [15] showed that vacancies could control the

operation of nanotube-based chemical sensors. Moreover, vacancy-type defects can impede the adsorption of quantum gases inside a bundle of carbon nanotubes [16], and give rise to irradiation-mediated pressure build-up inside nanotubes [17]. The defective nanotubes could be used as catalysts, and could facilitate thermal dissociation of water [18]. The dangling bonds can serve as a bridge of chemical connection between two tubes [23], or provide active sites for atomic absorption. The work of Ajayan et al. [8] showed that an ideal single vacancy in a (10, 10) tube is unstable: two of the three dangling bonds tend to form a new C–C bond, and the structure becomes a pentagonal ring coupling with one dangling bond, forming a so-called 5-1DB defect. Meanwhile, Krashennnikov et al. [21] indicated that there exists both a ground state and a metastable state for vacancies in a (10, 10) tube. These works mainly concentrated on the (10, 10) tube, although it is well-known that many properties of CNTs depend on their radius and chirality. Recently, Lu and Pan [24] showed that only the 5-1DB defect can exist in armchair carbon nanotubes, and that the formation energies depend on the radius of the CNTs. However, the transformation from single vacancy to its related point defects is not yet clear, and more scrupulous studies are needed.

In this work, we performed first-principles calculations to systematically investigate the structure and electronic properties of achiral SWNTs with ideal single vacancies. Our results indicate that the single vacancies in SWNTs

^a e-mail: wangcong00@mails.tsinghua.edu.cn

are unstable, and that they could transform into two possible point defects under certain conditions, in both armchair and zigzag SWNTs. The related point defects can be formed with no constraints, and the electronic structures of the point defects were investigated. The rest of the paper is organised as follows: the model and method are described in Section 2; results and analysis are presented in Section 3; and in Section 4, we present our conclusion.

2 Model and methods

We have performed ab-initio, total-energy calculations using VASP (the Vienna ab initio simulation package) [25,26], which is based upon an iterative solution of the Kohn-Sham equations of density-functional theory, using a plane-wave basis set with Vanderbilt ultrasoft pseudopotentials [27]. We employed a cutoff energy of 400 eV for the plane-wave basis set. For the exchange-correlation energy, we used the generalised-gradient approximation due to Perdew and Wang [28]. Brillouin-zone integrations were performed on a $1 \times 1 \times 4$ Monkhorst-Pack grid [29]. The energy minimisation was performed over the atomic and electronic degrees of freedom by using conjugate-gradient iterative techniques.

In our calculations, two groups of SWNTs were considered: a series of $(n,0)$ tubes with $n = 6-12$ containing 144–288 atoms, and a series of (n,n) tubes with $n = 3-9$ containing 120–360 atoms. For the $(n,0)$ tubes, we considered six unit cells in the supercell, and the length of the supercell along the tube axis is 25.56 Å. For the (n,n) tubes, the supercell contained ten unit cells, with a supercell length of 24.60 Å. We adopted supercell models in which the SWNTs were arranged with their outer walls separated by 6.00 Å.

3 Results and analysis

We first considered the case of $(n,0)$ CNTs, and selected a $(9,0)$ tube for study. An ideal single vacancy is made in a $(9,0)$ tube (Fig. 1a) by removing one carbon atom from the perfect SWNT, leaving three dangling bonds around the ideal vacancy. We investigated this single-vacancy system and found that the atoms around the vacancy experience large forces, hence we believe that such a system is unstable and does not represent the true atomic structure. In order to get the optimised structure of $(n,0)$ CNTs with an ideal vacancy, we performed full relaxation. We found that the C1 and C2 atoms (as labelled in Fig. 1a) tend to form a C–C bond, with this new bond directed perpendicular to the tube axis. The local structure around the ideal vacancy consists of one pentagonal ring and one dangling bond on atom C3, representing a 5-1DB-P [24] defect. The relaxation may have brought the geometry into a local minimal configuration, and so we considered another configuration involving the bonding of atoms C1 and C3. As shown in Figure 1, we manually set the distance between C1 and C3 to be 1.50 Å, and then fixed

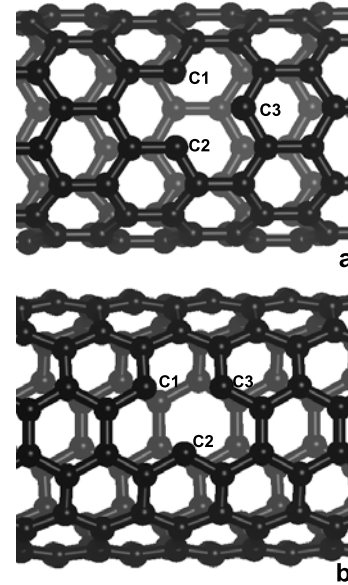


Fig. 1. (a) The structure of a $(9,0)$ zigzag CNT, where C1, C2, and C3 are the three atoms around the vacancy. (b) The structure of an ideal single vacancy in a $(6,6)$ armchair CNT.

atoms C1 and C3, while relaxing the remaining atoms in the system. After that, we performed full relaxation over the entire system. The final structure shows that the C1 and C3 atoms also form a C–C bond, tilted with respect to the tube axis. This structure is named the 5-1DB-T [24] defect. The C1–C3 and C2–C3 bonds are symmetrically equivalent.

Furthermore, we modelled many other zigzag carbon nanotubes. After extensive calculations, we found that the basic distortion patterns around vacancies in these tubes are almost the same as in the $(9,0)$ tube described above. The major difference between different zigzag tubes was the bond length of the new C–C bonds, both for 5-1DB-P and 5-1DB-T defects. This result agrees qualitatively with Lu's work [24], in both the geometrical structures and the formation energies. In Lu's work, the formation energies of zigzag CNTs behave like step and sawtooth features with nanotube radius for 5-1DB-P and 5-1DB-T defects, while in our calculations the formation energies only behave as step-like features, as shown in Figure 2a. This disagreement may come from the different methods of calculation; in Lu's work, they used a tight-binding model, while we used an ab initio method and are convinced that our calculation should be more accurate. The formation energy is defined as follows:

$$E_{\text{formation-energy}} = E_{\text{defect}} - E_{\text{perfect}} \times \frac{N_{\text{defect}}}{N_{\text{perfect}}}.$$

E_{defect} and E_{perfect} are the total energies of the defective and perfect systems, respectively, while N_{defect} and N_{perfect} are the number of atoms in the defective and perfect systems.

We treated armchair CNTs in a similar way to the zigzag CNTs. After removing one carbon atom from the SWNTs, we performed full relaxations. For $n = 3-6$,

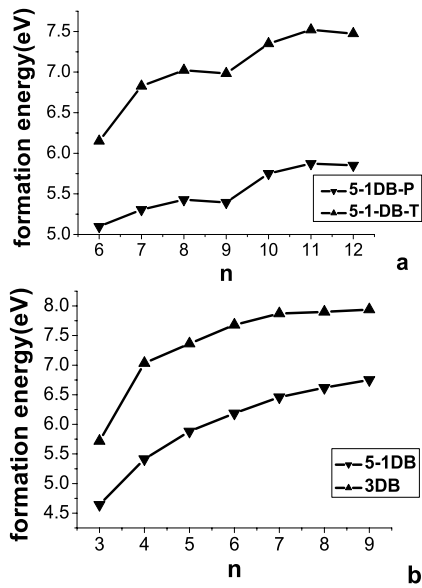


Fig. 2. Defect formation energies as a function of index n for (a) zigzag, and (b) armchair carbon nanotubes.

the three dangling bonds around the vacancy formed the 3DB defect, as in graphite. In the case of $n = 7-9$, atoms C1 and C2 (as labelled in Fig. 1b) formed a C-C bond, and this structure is named the 5-1DB defect [8]. We manually created the 5-1DB defect for the $n = 3-6$ SWNTs; we placed atoms C1 and C2 at a separation of 1.50 \AA , and fixed atoms C1 and C2 before relaxing the other atoms. After this, we allowed relaxation over the entire system, and obtained the optimised structure. For the systems of $n = 7-9$, we placed atoms C1, C2, and C3 in the exact positions as those in the 3DB defects in the $n = 3-6$ CNTs, and fixed these three atoms while relaxing all other atoms. After that, relaxing the entire system resulted in a metastable state; we describe 3DB defects as metastable states because of their higher total energies compared to the 5-1DB defects, and because 3DB can exist with no constraints. For all of the armchair carbon nanotubes considered, we found two types of optimised structure, and both of them are stable. We found the formation energy of a (4, 4) armchair CNT to be 5.41 eV , this value being quite close to the result of 5.31 eV found in other work [30]. In addition, the bond lengths that we obtained agree well with the work of Berber et al. [31].

As the stable states for each tube are found, the relative energetic stabilities of these point defects should be calculated, hence we evaluated the defect formation energies. Figure 2a shows the formation energies of 5-1DB-P and 5-1DB-T for zigzag CNTs, while Figure 2b shows the formation energy of 5-1DB and 3DB for armchair CNTs. It is clear that the formation energies obey $E_{(5-1DB-T)} > E_{(5-1DB-P)}$ for zigzag CNTs, and $E_{(3DB)} > E_{(5-1DB)}$ for armchair CNTs. Therefore, we suggest that 5-1DB and 5-1DB-P are the ground states for single-vacancy defects in armchair and zigzag CNTs, respectively, and that 3DB and 5-1DB-T are metastable states. For armchair CNTs, two carbon atoms in the 5-1DB defects form covalent

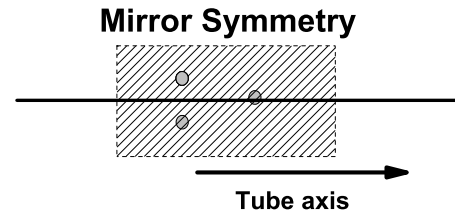


Fig. 3. Qualitative picture for a defect that has mirror symmetry through the tube axis.

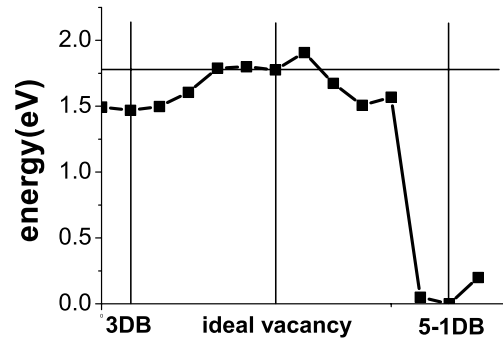


Fig. 4. The energy path from the 3DB ideal vacancy to the 5-1DB defect. The x -axis represents the transitional configurations, and the y -axis represents their relative energies (where we define the total energy of the 5-1DB state to be zero). For finding the energy path from the ideal vacancy to the 3DB defect, we first place atoms C1 and C3 at a separation of 2.56 \AA , which is equal to the separation of C1 and C3 in the 3DB defect. Then we move atom C2 towards the C1-C3 line using a step length of 0.10 \AA , and hence obtain the energy pathway of forming the 3DB defect from an ideal vacancy. Similarly, we fix atom C1 and move C3 (using a step length of 0.10 \AA) from the ideal vacancy position to the configuration representing the 5-1DB defect, and then move atom C2 using the same step length, in order to obtain the energy path for forming the 5-1DB defect from an ideal vacancy.

bonds, while 3DB defects contain three dangling bonds, explaining the higher energies of the 3DB defects. For zigzag carbon nanotubes, as shown in Figure 3, the single vacancy lies in the middle of the tube, hence it is easier to form a structure that has mirror symmetry through the tube axis than a structure that has no symmetry. The formation energy curves for zigzag tubes exhibit step-like features; interestingly, the step-like curve is periodic, and characterised by lower formation energies for defective $(n, 0)$ tubes with $n = 3k$ (where k is an integer) than for their neighbouring $(n-1, 0)$ and $(n+1, 0)$ tubes. This periodic property is not a unique phenomenon; in previous work [32], “band-folding” considerations and study of the relationship between the symmetry and the electronic structure for perfect tubes [33] suggested that perfect $(n, 0)$ tubes should be sorted into metals and semiconductors. The periodic variation in the electronic structure characteristics of the $(n, 0)$ tubes is governed by that of the metallic $(n, 0)$ tubes. All of the phenomena mentioned above are distinct in special properties, but similar in

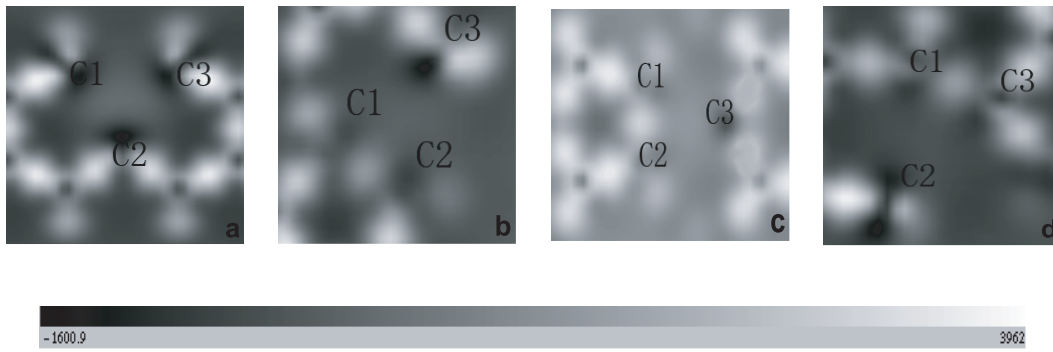


Fig. 5. Charge-density difference plots for: (a) the 3DB, (b) 5-1DB, (c) 5-1DB-P, and (d) 5-1DB-T arrangements, clearly showing the electronic structure of these point defects. These defect states can be identified using both the bond length and the charge-density differences. Here, the charge density difference is equal to the self-consistent charge density of the defect structure minus the charge density of isolated atoms.

periodic features. Figure 2b clearly shows that the formation energies for armchair CNTs increase smoothly with the radius of the tube. The formation energies for the 3DB defect converge towards a constant as the nanotube radius get larger, because the wall of the tube becomes flatter, and for very large tube radii the structures of the defects get closer to those in graphite.

We examined the bond lengths in the vacancy-related point defects, and the trend of the bond length shows the same features as the associated formation energies, except for the 3DB states, since these are metastable states and the carbon atoms do not tend to form C–C bonds.

For both armchair and zigzag CNTs, there are two kinds of point defect. In reference [24], the energy barrier for zigzag SWNTs is given as being lower than 1.9 eV. Our calculations reveal that for the armchair CNTs ($n = 3-6$), the initial structures that contain single vacancies do not directly convert to the most favoured configuration (5-1DB), but rather go via a metastable 3DB state. Could this phenomenon be attributed to the energy barrier between these two configurations? How much energy is associated with conversion of a 3DB defect, via the ideal vacancy, to the 5-1DB defect? (The ideal vacancy is formed by removing one carbon atom from the perfect tube.) In practice, searching for the general lowest energy pathway is prohibitive. Therefore, we selected only the (6,6) tube as an example. Starting from the ideal vacancy, we moved atoms C1, C2, and C3 towards the configurations of the various point defects. At each step, we fixed the three atoms surrounding the vacancy and relaxed all other atoms, and eventually obtained the energy path for defects transforming. Figure 4 shows the energy pathway corresponding to breaking the 3DB defect and forming an ideal vacancy, and then breaking the ideal vacancy and forming the 5-1DB defect. The x -axis represents the transition path, and the y -axis represents the relative energies. The energy barrier is defined as follows: $E_{\text{barrier}} = E_{\text{max}} - E_{\text{idealvacancy}}$, where E_{max} is the highest energy found in the related energy paths (ideal vacancy to 3DB and ideal vacancy to 5-1DB). The energy barrier in a realistic transition between the ideal vacancy and 3DB states should be no more than 22.8 meV, while the

energy barrier between the ideal vacancy and the 5-1DB defect should be less than 131.2 meV. It should be pointed out that we have manually assumed the pathway, hence the precision of these values might not be reproduced in experiment, although the physical picture is reliable. We have used the relationship: $k_B T = \Delta E_{\text{total}}$ to estimate the temperature needed to form 5-1DB from an ideal vacancy, and find that $T \approx 1500$ K, which is close to the result attained in reference [22], while $T \approx 260$ K is required for the 3DB defect.

Our work shows that the distortions caused by the point defects considered are spatially localised to within two shells of atom. None of the point defects considered in our calculation could effectively alter the σ -like- π -like hybridisation of the entire system [24]. The atomic-structure effect could be confirmed by the atomic configuration of the system. The C–C bond length returns to 1.42 Å (which is the ideal C–C bond length in a perfect tube) at a distance two atomic shells away from the vacancy. The electronic structure around the defects can be seen clearly in Figure 5, which shows the deformation density that can be used to estimate the type of bonds present in the defect. In Figure 5, the dark-blue spheres denote carbon atoms, and their related charge-density differences are given according to the colour bar below the picture. For armchair CNTs, the 3DB defects consist of three atoms forming three dangling bonds. The charge left in the middle of the defect comes entirely from the charge density of an isolated atom, because the result of the self-consistent defect calculation shows that there is essentially no charge present in this region. For the 5-1DB, 5-1DB-P, and 5-1DB-T defects, the atoms around the vacancies tend to form a new C–C bond and leave one dangling bond, and the charge density difference is strongly localised on the new C–C bonds, explaining the bonding character of the point defects. Therefore, our calculations accurately show the manner in which the three atoms join together, not only through the bond lengths or geometrical structures, but also through the electronic structures. When a single vacancy is created in a SWNT, the original σ -like- π -like hybridisation around the vacancy is destroyed, introducing constraints. The formation of bonds can lower the

energies of ideal vacancies and drive a change in their local structures into those of their related point defects.

4 Conclusion

To summarise, we have systemically studied single vacancies and their related point defects in achiral carbon nanotubes. Our calculations show that the ideal single vacancy is unstable and will reconstruct without constraint. For both armchair and zigzag SWNTs, ideal single vacancies can transform into either ground-state or metastable-state structures. The formation energies of zigzag CNTs change in a step-like fashion with the radius of the tubes, while the formation energies of the armchair CNTs change smoothly with the tube radius. In particular, in the case of 3DB defects, the formation energies tend towards a constant value as the nanotube radius get larger. The trends seen in formation energies are associated with the strengths of the new bonds around the point defects.

Cong Wang is indebted to Profs. Jian Wu, Shan-Ying Wang, and Dr. Zheng-Zheng Chen for their invaluable help. This work is supported by the NSFC (90306016).

References

1. Iijima, Sumio, Nature **354**, 56 (1991)
2. H. Noriaki, S. Sawada, A. Oshiyama, Phys. Rev. Lett. **68**, 1579 (1992)
3. A.N. Andriotis, M. Menon, D. Srivastava, L. Chernozatonskii, Phys. Rev. Lett. **87**, 066802 (2001)
4. A. Bezryadin, A.R.M. Verschueren, S.J. Tans, C. Dekker, Phys. Rev. Lett. **80**, 4036 (1998)
5. S.S. Fan, M.G. Chapline, N.R. Franklin et al., Science **283**, 512 (1999)
6. J.P. Lu, Phys. Rev. Lett. **79**, 1297 (1997)
7. L. Vitali, M. Burghard, P. Wahl et al., Phys. Rev. Lett. **96**, 086804 (2006)
8. P.M. Ajayan, V. Ravikumar, J.-C. Charlier, Phys. Rev. Lett. **81**, 1437 (1998)
9. L.C. Venema, J.W. Janssen, M.R. Buitelaar et al., Phys. Rev. B **62**, 5238 (2000)
10. M. Menon, Phys. Rev. Lett. **79**, 4453 (1997)
11. H.J. Choi, J. Ihm, S. Louie, M. Cohen, Phys. Rev. Lett. **84**, 2917 (2000)
12. C. Gómez-Navarro, P.J. DE Pablo et al., Nature Materials **4**, 534 (2005)
13. M. Sammalakorpi, A. Krasheninnikov, A. Kuronen et al., Phys. Rev. B **70**, 245416 (2004)
14. T. Belytschko, S.P. Xiao, G.C. Schatz, R.S. Ruoff, Phys. Rev. B **65**, 235430 (2002)
15. J.A. Robinson, E.S. Snow et al., Nano Letters **6**, 1747 (2006)
16. M.C. Gordillo, Phys. Rev. Lett. **96**, 216102 (2006)
17. L. Sun, F. Banhart, A.V. Krasheninnikov et al., Science **312**, 1199 (2006)
18. M.K. Kostov, E.E. Santiso, A.M. George et al., Phys. Rev. Lett. **95**, 136105 (2005)
19. Y. Zhu, T. Yi et al., Appl. Surf. Sci. **137**, 83 (1999)
20. A.V. Krasheninnikov, K. Nordlund, Surf. Sci. **454**, 519 (2000)
21. A.V. Krasheninnikov et al., Phys. Rev. B **63**, 245405 (2001)
22. A.V. Krasheninnikov, K. Nordlund, J. Vac. Sci. Technol. B **20**, 728 (2002)
23. M. Terrones1, F. Banhart, N. Grobert et al., Phys. Rev. Lett. **89**, 075505 (2002)
24. A.J. Lu, B.C. Pan, Phys. Rev. Lett. **92**, 105504 (2004)
25. G. Kresse, J. Furthmüller, Phys. Rev. B **54**, 11169 (1996)
26. G. Kresse, J. Hafner, Phys. Rev. B **47**, RC558 (1993)
27. D. Vanderbilt, Phys. Rev. B **41**, 7892 (1990)
28. J.P. Perdew, Y. Wang, Phys. Rev. B **45**, 13244 (1992)
29. H.J. Monkhorst, J.D. Pack, Phys. Rev. B **13**, 5188 (1976)
30. A.V. Krasheninnikov, P.O. Lehtinen, A.S. Foster et al., Chem. Phys. Lett. **418**, 132 (2006)
31. S. Berber, A. Oshiyama, Physica B **376–377**, 272 (2006)
32. X. Blase et al., Phys. Rev. Lett. **72**, 1878 (1994)
33. C.T. White et al., Nature **394**, 29 (1998)